8102 *Macromolecules* **2009**, *42*, 8102–8111
DOI: 10.1021/ma901442j

Macromolecules
ARTICLE

Synthesis and Properties of Amphiphilic Poly(1,4-Phenylene Ethynylene)s Bearing Alkyl and Semifluoroalkyl Substituents

Kathy B. Woody, Rakesh Nambiar, Glen L. Brizius, and David M. Collard*

School of Chemistry and Biochemistry, Georgia Institute of Technology, Atlanta, Georgia 30332-0400

Received July 3, 2009; Revised Manuscript Received August 24, 2009

ABSTRACT: New poly(1,4-phenylene ethynylenes)s (PPEs), in which each phenylene unit is substituted with both semifluoroalkoxy ($-O(CH_2)_m(CF_2)_nF$) and dodecyloxy ($-O(CH_2)_{12}H$) groups, are amphiphilic by virtue of the self-aggregating properties of the dissimilar side chains. Sonogashira polymerization of 4-iodophenylacetylenes bearing semifluoroalkoxy and alkoxy groups in the 2- and 5-positions, respectively, affords polymers with regular relative placement of the dissimilar side chains (i.e., "regioregular" materials containing only "head-to-tail" diads). This provides a Janus type structure. The assembly of these polymers was studied as a function of the length of the fluoroalkyl segment in the side chain by X-ray diffraction, differential scanning calorimetry, and UV−vis spectroscopy. The properties of these polymers were compared to analogues with random relative placement of side chains (i.e., materials containing a mixture of "head-to-head", "tail-to-tail" and "head-to-tail" diads), and to a nonfluorinated analogue. In contrast to the highly ordered and oriented solid phases formed by alkyl/semifluoroalkyl substituted poly(bithiophene)s, and despite their defined molecular structure, the amphiphilicity of the new semifluoro PPEs impedes their crystallization. While the overall structure of the regioregular polymer is amphiphilic, in which the dissimilar side chains are expected to segregate, we ascribe the lack of crystallinity to the disruption of side chain crystallization by virtue of having the alkyl and fluoroalkyl segments within a single side chain. These side chain cannot pack in an interdigitated fashion by virtue of the disparate segments, thereby leading to poorly ordered, or amorphous, solid materials.

Introduction

Poly(1,4-phenylene ethynylene)s (PPEs) have interesting properties resulting from their linear structure, strong fluorescence and solid state packing. This combination of properties has led to their use in a wide variety of applications including field effect transistors,[1] solar cells,[2] and sensors.[3] The substitution of PPEs with flexible side chains such as alkyl[4] or alkoxy[5,6] groups imparts solubility and crystallinity to the polymer. Variation of the structure of the side chains provides opportunities to tailor the optical and electronic properties of this versatile class of polymers.

The side chains influence the molecular packing of the PPE backbone in the solid state, and thereby alter the electronic structure of the close-packed conjugated systems. Taking a lead from nature, the design of amphiphilic structures allows for the manipulation of the packing and orientation of molecules in the solid state and at interfaces.[7] There are several examples of facially amphiphilic (i.e., "Janus-type") PPEs in the literature which have a combination of a hydrophobic alkyl side chain and a polar,[8] PEG[9,10] or cationic[11] side chains. These studies reveal that the interactions of the disparate side chains affect the molecular assembly of the polymers and their optoelectronic properties. While the segregation of these amphiphilic side chains affords the opportunity to influence molecular packing of conjugated polymers, the incorporation of hydrophilic side chains renders the materials sensitive to moisture.

Fluoroalkanes and hydrocarbons phase separate. On a molecular scale, fluoroalkyl and alkyl segments of a small molecule or a polymer segregate to afford control over molecular packing. Unlike other common combinations of side chains which give rise to amphiphilicity (e.g., alkyl, ionic, oligoether, siloxyl), hydrocarbon and fluorocarbon segments are both hydrophobic and are of similar size. The incorporation of semifluoroalkyl side chains in various polymers has led to enhanced thermal stability and chemical and oxidative resistance,[12−14] and formation of self-assembled architectures.[15−18] We have previously shown that poly(3-alkylthiophene)s (PATs) substituted with alternating alkyl and semifluoroalkyl side chains along the backbone adopt an all-anti configuration, giving rise to a Janus-type amphiphilic structure. The ribbonlike conjugated backbone has fluoroalkyl groups on one side and alkyl side chains on the other in the solid state. The segregation of dissimilar side chains gives rise to a highly ordered (i.e., crystalline) material. In addition, by avoiding interaction of the two disparate side chains with the substrate the polymeric molecules self-orient, leading to a packing in which the conjugated backbone is perpendicular to the substrate.[19] To explore the role of such amphiphilicity on other classes of conjugated polymers we have recently prepared PPEs that are substituted with alkoxy and semifluoroalkoxy side chains.

Dialkoxy PPEs are typically prepared by cross-coupling of symmetrically substituted 2,4-dialkoxy-1,4-diiodobenzenes and 2,4-dialkoxy-1,4-diethynylbenzenes (i.e., AA and BB type monomers). If each monomer is substituted with a pair of dissimilar alkoxy groups this polymerization results in an irregular placement of side chains along the PPE backbone with formation of head−head, head−tail, and tail−tail diads. We have recently reported the preparation of the first regioregular asymmetrically substituted PPE by the cross-coupling of asymmetrically substituted 2,4-dialkoxy-4-iodophenylacetylenes (i.e., a single A-B type monomer containing both the ethynyl and iodo substituents).[20,21] This allowed us to compare the properties of

*Corresponding author. E-mail: david.collard@chemistry.gatech.edu.

 Published on Web 09/10/2009

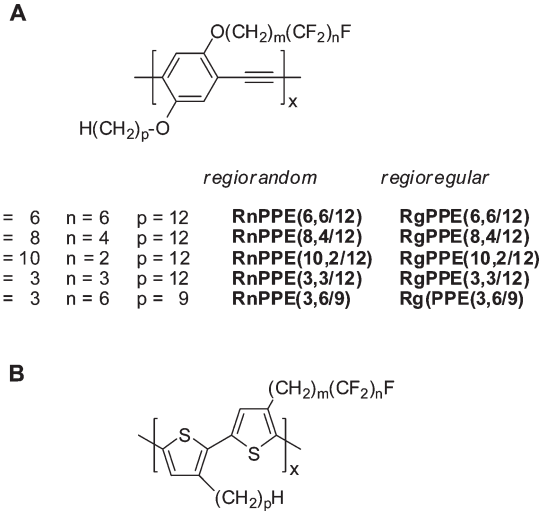

Figure 1. (A) Amphiphlic PPEs with semifluoroalkoxy and alkoxy side chains on each repeat unit. (B) analogous bithiophenes (ref 19).

head-to-tail regioregular and regiorandom polymers. However, these original polymers were limited to PPEs with different lengths of linear alkoxy side chains.

Here we extend this method to prepare amphiphilic regiorandom and regioregular PPEs bearing both semifluoroalkoxy ($-O(CH_2)_m(CF_2)_nF$) and alkoxy ($-O(CH_2)_pH$) side chains on each repeat unit, Figure 1, to explore the effect of amphiphilicity on the solid state assembly of the polymers. The hydrocarbon spacer ($(CH_2)_m$) of the semifluoroalkoxy chain insulates the conjugated polymer backbone from the electron-withdrawing inductive effects of the fluorocarbon segment. Accordingly, any changes in the electronic properties of the materials may be ascribed to changes in molecular packing arising from incorporation of fluoroalkyl segments and their relative placement, rather than an electronic substituent effect on the conjugated backbone. With the exception of **PPE(3,3/12)**, the semifluoroalkoxy and alkoxy side chains are the same length (where $m + n = p$), and are almost isosteric with symmetrically substituted dialkoxy PPEs (e.g., poly(2,4-dodecyloxy-1,4-phenylene ethynylene, **PPE(12/12)**).

Results and Discussion

Polymer Design: Amphiphilicity of Alkyl/Semifluoroalkoxyenzene. The aim of substituting each phenylene ring of PPE with alkoxy and semifluoroalkyloxy groups was to impart amphiphilicity so that the polymer adopts a Janus type structure leading to self-organization. 1-nonyloxy-4-(4,4,5,5,6,6,7,7,8,8,9,9,9-tridecafluorononyloxy)benzene serves as a small molecule model to illustrate the packing expected for the alkyloxy/semifluoro-alkoxy PPEs (e.g., **PPE(3,6/9)**). The unit cell of the single crystal X-ray structure of this compound, Figure 2, shows the clear segregation of the fluorinated and nonfluorinated side chains. The two types of side chains segregate so that they interact side-by-side and end-on-end with like side chains. This leads to a bilayer lamellar structure with a repeat distance of 54 Å, approximately twice the length of the conformation of a single molecule in an extended all-trans conformation. The benzene rings form stacks in the direction perpendicular to the view shown in Figure 2B.

Synthesis of PPEs. We envisaged a synthetic approach to asymmetrically substituted PPEs whereby semifluoroalkoxy chain would be incorporated into a monomer using a Mitsunobu etherification between suitably substituted phenols and commercially available semifluorinated alcohols. To explore the effect of variation of the fluoroalkyl chain

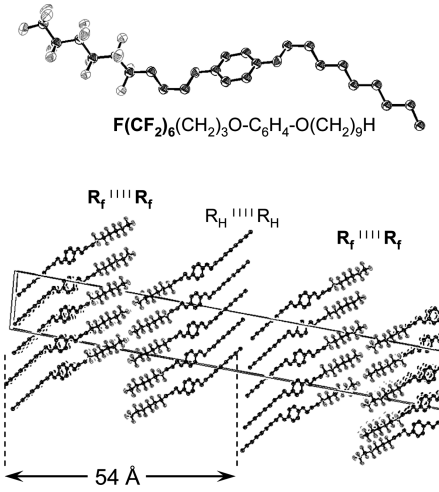

Figure 2. Amphiphilic 1-nonyloxy-4-(4,4,5,5,6,6,7,7,8,8,9,9,9-tridecafluorononyloxy)benzene: top, molecular structure; bottom, unit cell. Hydrogen atoms have been omitted for clarity.

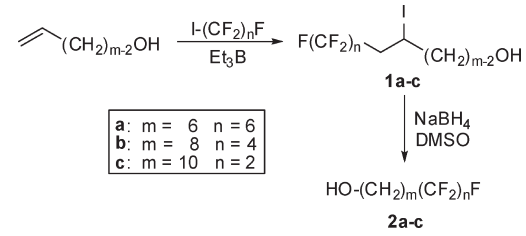

Figure 3. Synthesis of semifluoroalcohols.

length (n) while keeping the total length of the semifluoroalkoxy side chain constant (i.e., $m + n$), and therefore isosteric with the alkoxy substituent ($-O(CH_2)_pH$, $p = 12$ in most cases), we needed to develop a general route to semifluoroalcohols ($(HO-(CH_2)_m(CF_2)_nF$) where $m + n = 12$. They were successfully prepared by a radical addition reaction between a perfluoroalkyl iodide and ω-alken-1-ol, Figure 3. Initially, we explored the use of copper powder to facilitate the regiospecific addition of perfluoroalkyl iodides across the terminal alkene.[22] However, long reaction times were required to form only moderate yields ($< 60\%$), and the use of high temperatures required for this reaction presented a major limitation for the low boiling perfluoroethyl iodide (bp = 13 °C). Other common radical initiators such as $Pd(PPh_3)_4$,[23] dibenzoyl peroxide,[24] and AIBN[25] also require high temperatures and often give low yields. We chose instead to use triethylborane as a catalyst, which has been shown to catalyze the addition reaction at low temperatures, but which has not gained widespread use for the preparation of semifluorinated chains.[12,26,27] This method proved to be highly effective, resulting in quantitative addition of the perfluoroalkyl iodides to the ω-alken-1-ols to give the iodo-substituted semifluoroalcohols, **1**, at temperatures as low as −20 °C within 2 h. Conversion of **1** to the semifluoroalcohol **2** was achieved via reductive deiodination using sodium borohydride in dry DMSO.

A Mitsunobu reaction was used to install the semifluoroalkoxy chain onto 4-(dodecyloxy)phenol to afford the unsymmetrically substituted 1,4-dialkoxybenzenes **3**, Figure 4. Subsequent iodination of **3** yields the diiodinated monomers **4**. Palladium catalyzed coupling of TMS acetylene to **4**, followed by desilylation in the presence of tetra-*n*-butylammonium fluoride gave the diethynyl monomers **6**. The palladium catalyzed Sonogashira cross-coupling condensation

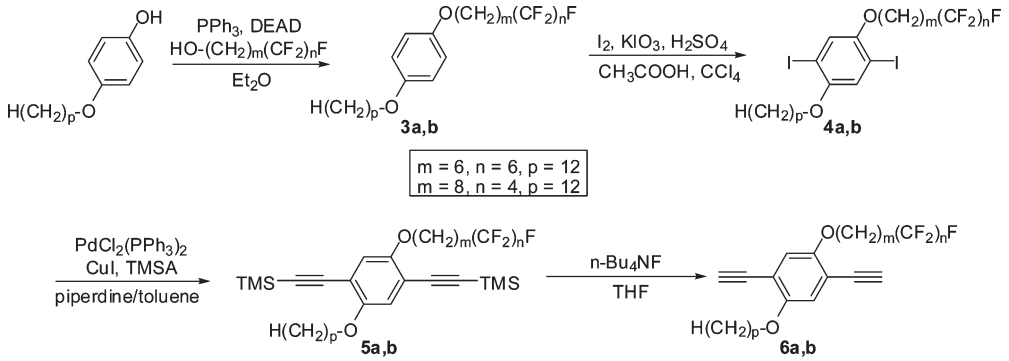

Figure 4. Synthesis of asymmetrically substituted diiodobenzenes **4** and diethynylbenzenes **6**: Monomers for the preparation of regiorandom PPEs.

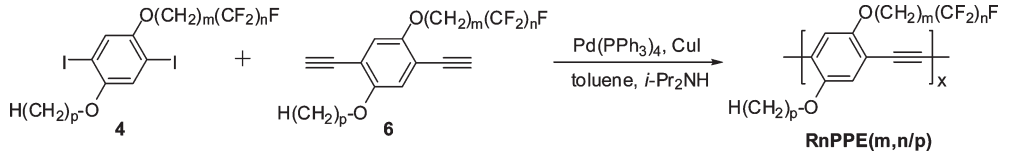

Figure 5. Preparation of regiorandom amphiphilic semifluoroalkoxy/alkoxy-substituted polymers, **RnPPE(*m,n*/*p*)**.

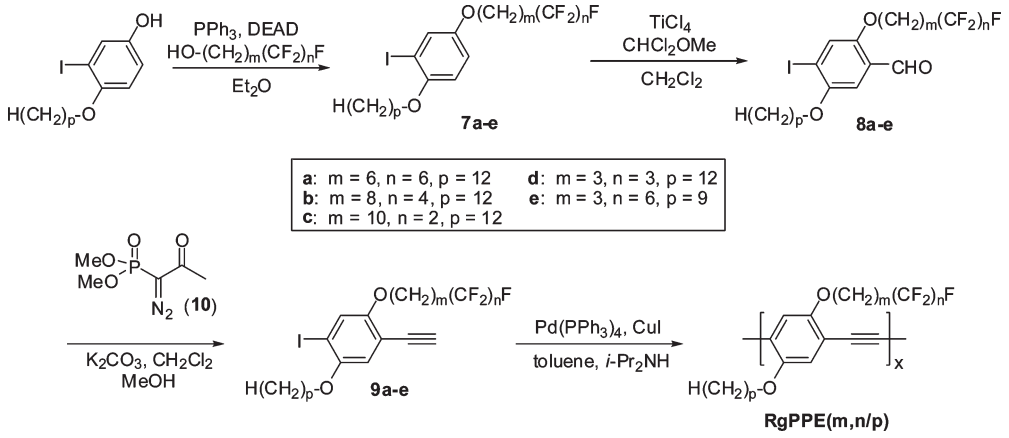

Figure 6. Synthesis of regioregular PPEs.

polymerization of diiodo (AA) and diethynyl (BB) monomers **4** and **6** produced the amphiphilic, regiorandom PPEs, Figure 5.

The synthesis of regioregular PPEs required a single monomer, **9**, bearing both an iodo and an ethynyl group (i.e., an AB monomer), Figure 6. The substitution pattern of the monomers was established by the regioselective iodination of 4-alkoxyphenols using previously reported methods to give 4-alkoxy-3-iodophenols.[21] A Mitsunobu reaction was then used to install the semifluoroalkyl side chains to provide **7a**−**c**. To generate the AB type monomer **9**, it was necessary to selectively place an ethynyl group para to the iodine of **7**. A formylation reaction produced benzaldehyde **8**, which was then transformed to alkyne **9** using the Bestman−Ohiro homologation (treatment with $(MeO)_2P(=O)C(=N_2)CO\text{-}CH_3$). While the formylation reaction was not completely regiospecific,[21] the desired 1,2,4,5-tetrasubstituted isomer was easily separable from the byproducts by column chromatography followed by recrystallization. The AB type monomer **9** was polymerized using the palladium catalyzed condensation polymerization to produce regioregular PPEs containing exclusively head-to-tail linkages.

Both regioregular and regiorandom PPEs were isolated and purified by precipitation from the reaction mixture by addition to a large volume of MeOH, followed by dissolution in chloroform and reprecipitation by addition to acetone, to give bright orange solids. Efforts to prepare PPEs from semifluoroalcohols with short carbon spacers ($m = 3$) afforded completely insoluble materials, thus **RgPPE(3,3/12)** and **RgPPE(3,6/9)** were not characterized further. The remaining polymers were wholly soluble in chloroform and THF, with the exception of **RgPPE(6,6/12)** of which only the chloroform soluble portion was used for characterization. An isosteric symmetrically substituted dialkoxy-PPE, poly(2,4-dodecyloxy-1,4-phenylene ethynylene), **PPE(12/12)**, was synthesized by polymerization of the di(dodecyloxy) substituted diiodo- and diethynylbenzene monomers.[21,28] The polymers were characterized by ^1H and ^{13}C NMR, FT-IR, and UV−vis absorption spectroscopies, differential scanning calorimetry (DSC), gel permeation chromatography (GPC), and X-ray diffraction (XRD).

Structural Characterization. The molecular weights of the PPEs were determined both by end group analysis and GPC, Table 1. The number-average molecular weights (M_n) could be determined by ^1H NMR spectroscopy by virtue of the distinct chemical shifts of the protons ortho to the iodo substituent (δ 7.3) and ethynylene group (δ 6.9) of the two end groups. PPEs synthesized from AB type monomers bear

Table 1. Physical Properties of RgPPE(m,n/p), RnPPE(m,n/p) and PPE(12/12) [a]

polymer	M_n[b,c] (kg mol^{-1})	M_n[b,d] (kg mol^{-1})	M_w[d,e] (kg mol^{-1})	PDI[d,f]	DP[c,g]	T_m[h] (°C)	ΔH (kJ mol^{-1})[i]
RgPPE(6,6/12)	8.4	9.0[j]	18	2.02	12	235	5.7
RnPPE(6,6/12)	15	k			21	215	3.6
RgPPE(8,4/12)	21	8.6[l]	17	2.03	33	198[m]	3.2
RnPPE(8,4/12)	19	18	38	2.13	30	198[m]	2.9
RgPPE(10,2/12)	13	36	88	2.41	24	194	2.1
PPE(12/12)	14	49	134	2.73	29	188	4.5

[a] **RgPPE(3,3/12)** and **RgPPE(3,6/9)** were insoluble in common organic solvents and were not characterized by these methods. [b] Number-average molecular weight (M_n). [c] Determined by end group analysis. [d] Determined by gel permeation using polystyrene standards. [e] Weight-average molecular weight (M_w). [f] Polydispersity index (PDI). [g] Degree of polymerization (phenyls as repeating units). [h] Melting temperatures (T_m) determined by DSC at a scan rate of 10 °C.min^{-1}. [i] kJ per mole of repeat unit. [j] Chloroform soluble portion only, fractionation occurred. [k] **RnPPE(6,6/12)** forms a gel in THF so its molecular weight cannot be determined by this method. [l] Not all of the polymer sample was soluble in THF; fractionation occurred. [m] **RgPPE(8,4/12)** and **RnPPE(8,4/12)** show a very broad thermal transition in the DSC measurement.

one end group of each type, as confirmed by the equal integrals of the two signals. Polymers prepared from coupling AA and BB type monomers have different amounts of these end groups, due to slight stoichiometric imbalances of the monomers in the polymerization reaction mixture. The degrees of polymerization (DP) range between 21 and 33 repeat units with the exception of **RgPPE(6,6/12)** which had a DP of only 12 as a result of poor solubility of the polymer in chloroform. However, the molecular weights of all of the PPEs in this study are higher than the effective conjugation length of PPEs (approximately 11 repeat units).[29] Regioregular **RgPPE(6,6/12)** and **RgPPE(8,4/12)** are much less soluble then their regiorandom counterparts, likely a result of higher crystallinity arising from their more regular structures.

Differences in the appearance of the aromatic region of the ^{1}H NMR spectra for **RgPPE(6,6/12)** and **RnPPE(6,6/12)** illustrate the regioregularity on the polymer structure. Three types of linkages can be formed when coupling AA and BB type monomers: head-to-tail (*ht*), head-to-head (*hh*), and tail-to-tail (*tt*), Figure 7.

The aromatic region in the ^{1}H NMR spectrum of **RgPPE-(6,6/12)** has two sharp singlets at δ 7.0 and δ 7.1 ppm, corresponding to the protons ortho to the alkyl and semifluoroalkyl chain, respectively, Figure 8B. However, only one broad signal is observed for the regiorandom analogue (Figure 8A) as a result of the overlap of peaks occurring for protons in different environments on the aromatic backbone arising from *hh*, *ht*, and *tt* diads.

Thermal Transitions. Thermal transition temperatures and enthalpies (ΔH) of the PPEs in this study were determined by differential scanning calorimetry (DSC), Table 1. A single endothermic peak is observed for each of the polymers upon heating, which is similar to the melting transition observed for symmetrically substituted dialkoxy−PPEs.[30] The transition temperatures all occur at higher temperatures than for the 2,4-(didodecyloxy)-substituted PPE, **PPE(12/12)**, (188 °C) and depend on the relative length of the fluorinated segment in the semifluoroalkoxy side chain. The temperature of the transition is highest for polymers with longer fluorinated segments (i.e., larger values of *n*). The thermal transition temperatures also depend on the regioregularity of the material. The regioregular **RgPPE(6,6/12)** has a significantly higher thermal transition than the regiorandom analogue, **RnPPE(6,6/12)** (235 versus 215 °C) in spite of having a lower molecular weight. The regioregular and regiorandom analogues of **PPE(8,4/12)** homologue have identical melting points (198 °C), although the transitions are very broad. The enthalpies of the transition (ΔH) provide additional insight into the effect of regioregularity. The enthalpies for the regioregular (**Rg**) analogues of both the (**6,6/12**) and (**8,4/12**) homologues are higher than for the corresponding regiorandom (**Rn**) analogues, demonstrating an increase in thermal stability of the crystalline phase of the regioregular homologues.

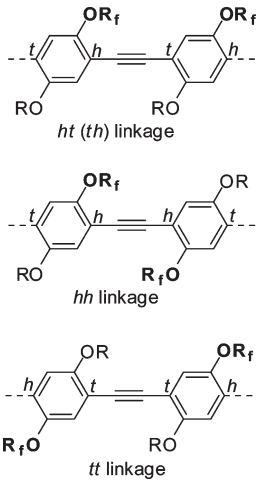

Figure 7. Three possible dyads occur when coupling AA and BB type monomers, where R_f = semifluoroalkoxy and R = alkoxy.

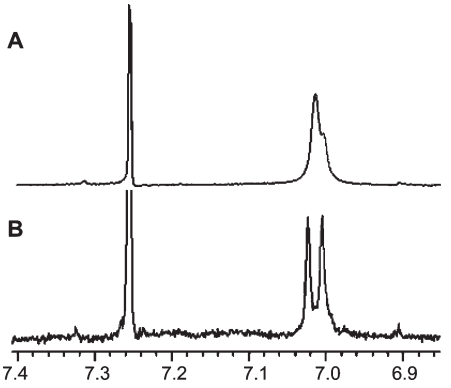

Figure 8. ^{1}H NMR spectra of **PPE(6,6/12)**: (A) regiorandom (**Rn**); (B) regioregular (**Rg**).

No thermal transitions are observed in the cooling scan in the differential scanning calorogram; the lack of an exothermic peak indicates that the material does not crystallize on the time scale of the cooling scan. Reheating the sample reveals the absence of cold crystallization and no melting transition. Annealing the samples just below the T_m, cooling and reheating does not reveal an endothermic transition, nor does letting the samples sit at room temperature for several weeks. The lack of thermal transitions after first melting is not due to thermal degradation, as supported by the ability to redissolve the PPE samples in chloroform, and the unchanged IR and ^{1}H NMR spectra of the samples.

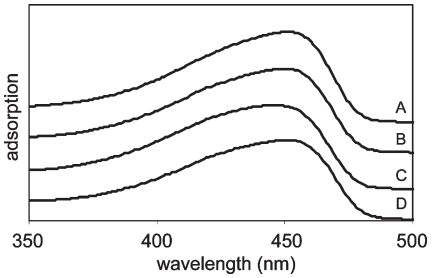

Figure 9. Solution UV−vis absorption in $CHCl_3$: A, RnPPE(8,4/12); B, RgPPE(8,4/12); C. RgPPE(10,2/12); D, PPE(12/12).

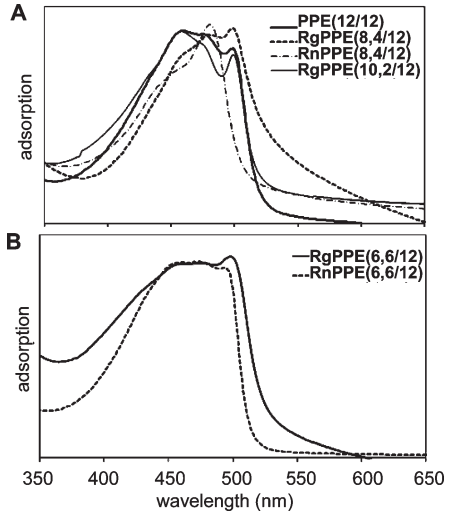

Figure 10. UV−vis spectra of annealed thin films of PPEs: A, symmetrically substituted **PPE(12/12)**, regioregular and regiorandom analogues of **PPE(8,4/12)** and **RnPPE(10,2/12)**; and B, regioregular and regiorandom analogues of **PPE(6,6/12)**.

Electronic Spectra. UV−vis absorption spectra were obtained for regioregular and regiorandom analogues of the amphiphilic alkoxy/semifluoroalkoxy-PPEs both in solution and as thin films. The absorption spectra for the PPEs in solution all show a broad absorption at around 450 nm, which is also characteristic of the symmetrically substituted dialkoxy-PPEs, Figure 9. The similarity of these spectra can be attributed to the low rotational barriers of PPEs in solution (estimated to be < 1 kcal/mol),[31] and lack of aggregation of the polymer chains in $CHCl_3$ solution.

Larger differences were observed between the spectra of thin films of the materials, Figure 10. Films were prepared by drop-casting a chloroform solution of the polymers (approximately 0.1 mg.mL^{-1}) onto glass slides, allowing the solvent to evaporate. The films were then annealed at 110 °C under vacuum for 24 h. The symmetrically substituted **PPE(12/12)** (solid line in Figure 10A) has an absorption with contributions at 460, 480, and 500 nm. Peaks at these wavelengths also contribute to the absorption of the amphiphilic alkoxy/semifluoroalkoxy−PPEs. Whereas for **PPE(12/12)** the peak at the lowest wavelength is the strongest, it is the peak at highest wavelength that is strongest for the regioregular homologues of **PPE(6,6/12)**, **PPE(8,4/12)**, and **PPE(10,2/12)**. The peak at 500 nm is absent in the spectrum of the regiorandom analogue **RnPPE(8,4/12)**, Figure 10A, and relatively weak in the spectrum of **RnPPE(6,6/12)**.

We attribute the peak at higher wavelength to a portion of the materials that has a greater conjugation length arising from a more ordered, planar structure. The symmetrically substituted alkoxy−PPEs (e.g., **PPE(12/12)**) form a planar, highly conjugated structure by virtue of side chain crystallization of the regularly placed linear alkoxy chains (Figure 11A). The observation that the regioregular materials give a stronger absorption at 500 nm suggests that these films have a higher portion of the most highly conjugated material. For the regiorandom analogues the absence of a peak at 500 nm arises from the irregular placement of alkoxy and semifluoroalkoxy This irregularity hinders side chain crystallization (Figure 11B, left). While rotation of individual repeat units around the polymeric main chain allows the dissimilar side chains to segregate (Figure 11B, right), this would result in steric hindrance between repeat units, thereby leading to a disordered structure and a hindrance of planarization.

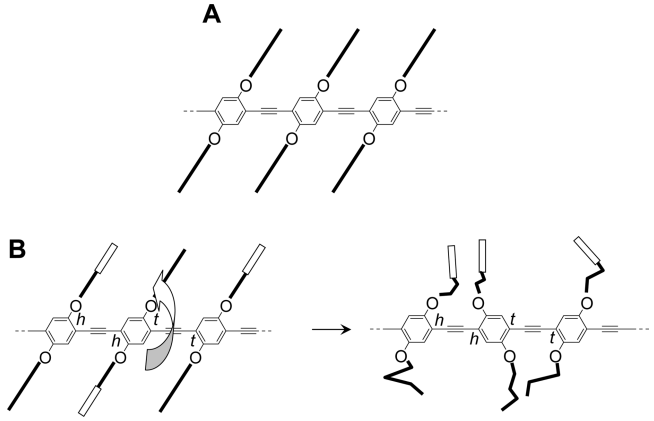

Figure 11. While regiorandom **RnPPE(*m*,*n*/*p*)** is isosteric with **PPE(*p*/*p*)**, amphiphilicity disrupts molecular packing. A, Side chain crystallization of symmetrically substituted dialkoxy-PPE, e.g., **PPE(12/12)**. B, In regiorandom amphiphilic analogue, crystalline packing of the side chains is impeded by packing of dissimilar chains (left); rotation about the backbone segregates the two types of side chains, but leads to steric hindrance, thereby disrupting molecular packing and inducing disorder.

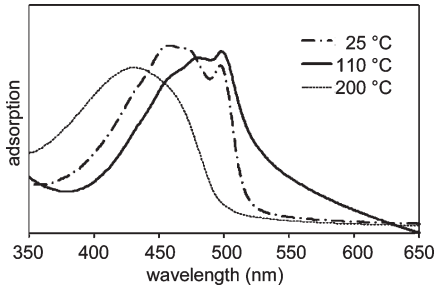

Figure 12. UV−vis absorption of thin films of **RgPPE(8,4/12)** at room temperature, before annealing (25 °C) and after heating at 110 and 200 °C for 2 h (mp = 198 °C).

The UV−vis absorption spectra of the PPEs are affected by annealing at different temperatures, Figure 12. Annealing **RgPPE(8,4/12)** at 110 °C for 12 h (i.e., below the melting temperature of 198 °C) and then cooling to room temperature results an increase in the intensity of the peak at 500 nm relative to the other peaks, indicating the formation of a more conjugated structure giving rise to absorptions at lower energy. Upon holding the sample just above the melting point at 200 °C and then cooling gives rise to a broad blue-shifted absorption with $\lambda_{max} = 433$ nm. Dissolving and recasting the film gives spectra identical to those of the original unannealed absorption samples. Thus, annealing a semicrystalline as-cast film results in an increase in the 500 nm absorption due to formation of greater amounts of the crystalline phase. However, cooling from the melt results

in an amorphous material that gives a blue-shifted absorption corresponding to a material with less conjugation. This agrees with the observation from the thermal analysis experiment that the materials cooled from the melt do not crystallize, even after extensive annealing.

Molecular Packing. The supramolecular structures of the amphiphilic semifluoroalkoxy/alkoxy-substituted PPEs in this study were characterized using wide-angle X-ray diffraction (WAXD). A film of **PPE(12/12)** was prepared by drop-casting a xylene solution onto a silicon substrate. However, attempts to process the amphiphilic PPEs using this method provided cracked and irregular films that were not suitable for X-ray diffraction. In order to overcome this problem, the silicon substrates were first modified with a self-assembled monolayer by treatment with either dodecyldimethylchlorosilane or (heptadecafluorodecyl)dimethylchlorosilane (see Supporting Information). Suitable films of **RgPPE(6,6/12)**, **RnPPE(6,6/12)** and **RgPPE(8,4/12)** could only be formed on slides modified with a fluoroalkyl monolayer, whereas **RgPPE(10,2/12)** and **RnPPE(8,4/12)** formed the best films on the alkylated surfaces. Thus, the interaction between the polymer and substrate has a strong influence on film quality, with polymers bearing fluorine-rich side chains forming better films on fluorous surfaces, and those with low content of fluorine form better films on the oleophilic alkylsilane monolayer.

X-ray diffraction experiments were performed on both pristine and annealed 100 μm-thick films. The WAXD patterns of the annealed amphiphilic PPEs and the symmetrically substituted **PPE(12/12)** are shown in Figure 13A−F. In each case, annealing the drop-cast films under vacuum at 110 °C for 24 h the peaks in the diffraction pattern become sharper and more resolved, but do not change in position, indicating an increase in crystallinity.

Symmetrically substituted **PPE(12/12)** shows a sharp first order diffraction peak at 25 Å, and less intense higher order reflections at 12.3, 8.4, and 5.0 Å, corresponding to the (100), (200), (300), and (500) reflections arising from a lamellar crystalline morphology.[32] There is a monotonic decrease in the size of the reflections with odd indices (i.e., (100), (300), (500)), and those with even indices (i.e., (200) and (400), which is not observed) are significantly weaker. Introducing amphiphilicity has a significant impact on the molecular packing of the PPEs. However, in contrast to the Janus type polythiophenes,[19] in which imparting amphiphilicity gave rise to highly ordered and oriented crystalline phases, this change in molecular structure disrupts the lamellar packing of the PPE backbone. The peaks in the diffractograms of all of the amphiphilic PPEs are broader than those of the isosteric **PPE(12/12)**. For the most part, the peaks which appear in the diffractograms of the amphiphilic PPEs correspond to peaks given by **PPE(12/12)**. For example, all of the diffractograms display a reflection at between 8.5 and 8.9 Å. However, none of the fluoroalkyl-substituted polymers show all of the reflections present in the symmetrical dialkoxy material. In addition, the relative intensities of peaks in the diffractogram of the amphiphilic are quite distinct from those in the symmetrical analogue. For example, in the diffractorgram of **RgPPE(10,2/12)** the peak at $d = 12.7$ Å is significantly stronger than those at $d = 24.7$ and 8.5 Å, the reverse of the situation for **PPE(12/12)**. Surprisingly, given the important role of regioregularity of side chain substitution of PATs and PPEs, the regiorandom materals (Figure 13, parts B and D) give stronger diffraction peaks than the corresponding regioregular materials (Figure 13, parts A and C). The diffraction peak at $d = 12.3$ Å is very weak for **PPE(12/12)**, but the diffractograms of **RgPPE-(10,2/12)** and **RnPPE(8,4/12)** have significant peaks in this region. The strong reflection at 25 Å in the diffractogram of **PPE(12/12)** is missing, or weak, for the other materials. The diffractograms of the amphiphilic PPEs which have been cooled to room temperature from the melt indicate a complete loss of crystallinity, consistent with DSC results.

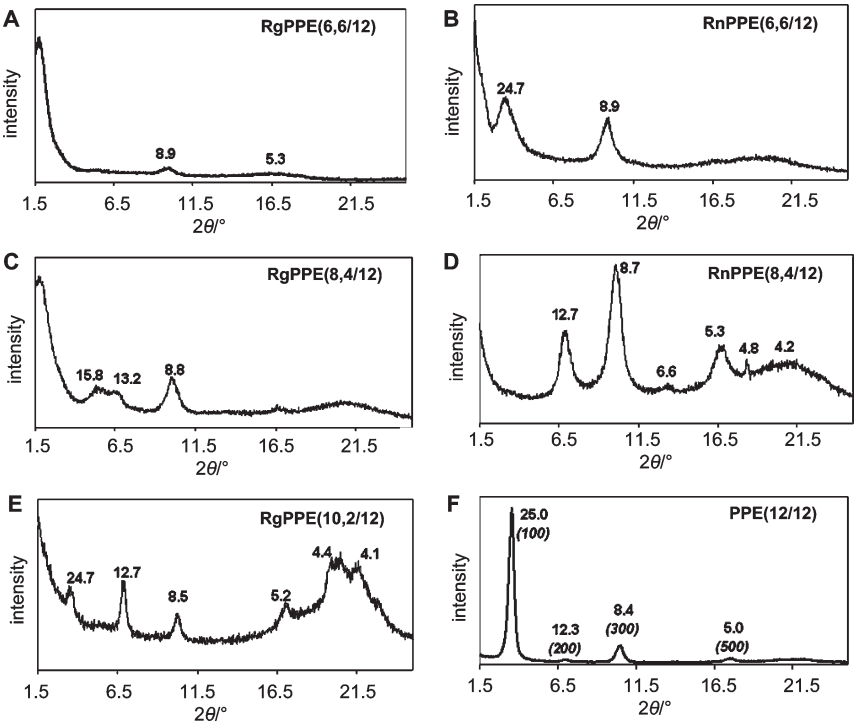

Figure 13. Wide angle X-ray diffraction patterns for annealed films: (A) **RgPPE(6,6/12)**; (B) **RnPPE(6,6/12)**; (C) **RgPPE(8,4/12)**; (D) **RnPPE(8,4/12)**; (E) **RgPPE(10,2/12)**; (F) **PPE(12/12)**. Peaks are labeled with *d* spacings in Å.

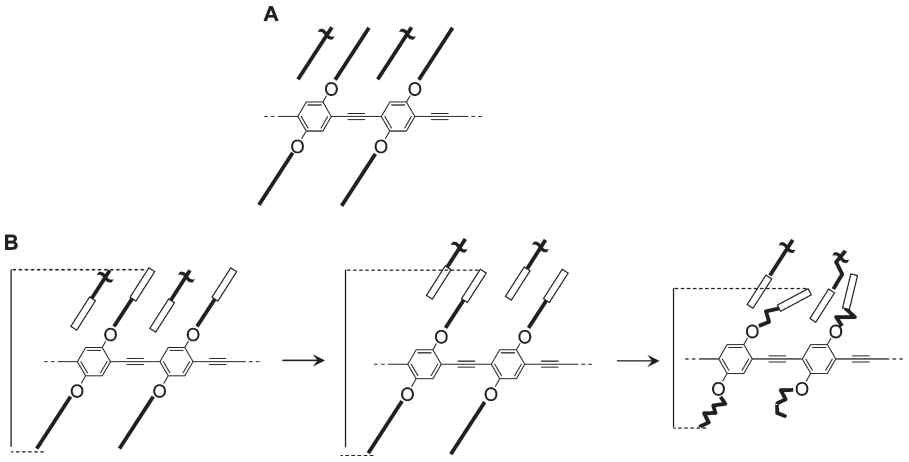

Figure 14. Incorporation of amphiphilic side chains imparts disorder to the structure of PPEs. (A) The side chains of symmetrically substituted dialkoxyl−PPEs, e.g., **PPE(12/12)** interdigitate to form a lamellar structure. (B) Aggregation of fluoroalkyl segments limited extent of interpenetration of side chains, requiring that the alkylene spaces, $(CH_2)_m$, undergo conformational disordering to fill space efficiently, thereby introducing molecular disorder.

The disordered nature of the amphiphilic PPEs is in contrast to similar facially amphiphilic Janus-type alkyl/semifluoroalky-substituted polybithiophenes.[19] The spacing between side chains on the PPE backbone leads to interdigitation of side chains on adjacent polymer chains, Figure 14A. However, similar interpenetration of the semifluoroalkyl chains would result in alkyl-fluoroalkyl contacts (Figure 14B, left). Segregation of the alkyl and fluoroalkyl segments would require that the side chains do not fully interdigitate. Thus, we postulate that a disordered structure is formed to accommodate the segregation of the side chains (Figure 14B, right).

The similarity of the *d*-spacings for the peaks of all members of the series of alkoxy/semifluoroalkoxy-substituted polymers, **PPE(*m*,*n*/12)**, to those in the diffractograms of the symmetrical isosteric analogue **PPE(12/12)** suggests that the amphiphilic materials form crystalline phases with a similar lamella packing. However, the relative intensities of the peaks in the diffractograms are quite distinct. The relative intensity of the peaks arises from the electron density profile within the unit cell (the electron density profile is the Fourier transform of the diffractogram.) The form of the electron density profile of a polyphilic polymers in a bilayer architecture is unusual compared to conjugated materials (i.e., semirigid polymer chains bearing a single type of alkyl side chain, e.g., **PPE(12/12)**,) and resembles that of a lipid bilayer.[33−35] The relative intensities of the peaks in the diffractogram relate to the relative size and electron density of the separate microenvironments formed by segregation of the alkylene spacers (*m*), semifluoroalkyl chains (*n*), alkyl chains (*p*), and 1,4-phenylene units (Figure 14). The simulation of the electron density profiles based on the diffraction data is currently under investigation.

Conclusions

A synthetic route to regioregular and regiorandom amphiphilic Janus-type PPEs bearing a semifluoroalkoxy and an alkoxy side chain on each phenyl ring has been described. Characterization of these amphiphilic PPEs reveals that thermal transitions in these polymers are affected both by the length of the fluorocarbon segment as well as regioregularity. In comparison to symmetrically substituted dialkoxy PPEs, the amphiphilic PPEs have a red-shifted optical absorption and no longer display a simple lamellar morphology, as indicated by the X-ray diffraction patterns. Annealing the polymers above the melting temperature leads to a blue-shifted optical absorption and loss of all crystallinity. Thus, the alkoxy/semifluoroalkoyl-substitution pattern of the amphiphilic PPEs impedes crystallization. This is in contrast to the highly ordered and oriented solid phases formed by alkyl/semifluoroalkyl-substituted poly(bithiophene)s. The difference in the behavior of these polymers may arise from the extent to which the side chains of dialkoxy−PPEs interdigitate. Segregation of the dissimilar side chains of the amphiphilic PPEs impedes this interdigitation and thereby disrupts crystallization.

Experimental Section

All starting materials were purchased from commercial sources and used without further purification unless stated otherwise. THF and Et_2O were dried over sodium benzophenone ketyl prior to distillation under argon. Column chromatography was performed on flash grade silica (32−60 Å, Sorbent Technologies, Atlanta, GA). Thin-layer chromatography was performed on 3 × 5 cm silica gel plates (0.2 mm thick, 60 F254) on an aluminum support (Sorbent Technologies). NMR analysis was performed on a Bruker DSX 400 or DSX 300 instruments using $CDCl_3$ as the solvent unless stated otherwise. Chemical shifts are reported relative to internal tetramethylsilane. IR analyses were performed on a Nicolet 4700 FTIR with an ATR attachment from Smart-Orbit Thermoelectronic Corporation. Ultraviolet−visible analysis was performed on a Perkin-Elmer Lambda 19 spectrophotometer. Elemental analyses were performed by Atlantic Microlab, Inc. (Norcross, GA). The Bestman-Ohiro reagent (**10**) was prepared using previously reported methods.[36] Syntheses of analogues **a** ($m = 6$, $n = 6$, $p = 12$) are described below. Homologues **b** ($m = 8$, $n = 4$, $p = 12$), **c** ($m = 10$, $n = 2$, $p = 12$), **d** ($m = 3$, $n = 3$, $p = 12$), and **e** ($m = 3$, $n = 6$, $p = 9$) were synthesized using similar procedures unless otherwise stated. Spectral characterization of homologues **b**, **c**, **d**, and **e** is provided in the Supporting Information.

7,7,8,8,9,9,10,10,11,11,12,12,12-Tridecafluoro-5-iodododecan-1-ol, 1a. *Cu-Catalyzed Method.* A mixture of 5-hexen-1-ol (4.4 mL, 37 mmol), 1-perfluorohexyl iodide (25 g, 56 mmol) and Cu powder (0.36 g, 5.7 mmol) was heated to 120 °C for 24 h in a sealed thick-walled glass vessel under argon. Et_2O (50 mL) was added and the Cu catalyst was removed by filtration. The solvent was removed under reduced pressure and the residue was subjected to flash column chromatography (silica gel, 20:80 v/v ethyl acetate:hexanes) to afford **1a** as a colorless liquid (9.91 g, 49%). ^{1}H NMR (300 MHz, $CDCl_3$): δ 4.27−4.36 (m, 1H, C5 CH), 3.65 (t, $^3J_{HH} = 6$ Hz, 2H, $-OCHH_2-$), 2.66−3.01 (m, 2H, C6 CH_2), 2.02 (br s, 1H, −OH), 1.47−1.87 (m, 6H). ^{13}C NMR

(75 MHz, $CDCl_3$): δ 62.44 (C1), 41.59 (t, $^3J_{CF}$ = 20 Hz, C6), 40.00, 31.49, 25.97, 20.44. IR (ATIR): 3350 (br, O−H str), 2947, 2884, 1749, 1367, 1195 (C−O str), 1144, 1063, 812, 735, 698, 658, 509 cm^{-1}.

BEt_3-Catalyzed Method. A mixture of 5-hexen-1-ol (5.5 mL, 47 mmol) and 1-perfluorohexyl iodide (25 g, 56 mmol) was cooled to 0 °C under argon, and BEt_3 (2 mL, 2 mmol, 1 M in hexanes) was added via syringe. The mixture was stirred at 0 °C for 3 h, and MeOH (5 mL) was added, followed by H_2O (50 mL). The mixture was extracted with hexanes (200 mL) and dried over $MgSO_4$. The solution was filtered through a pad of silica gel (1:5 v/v EtOAc:hexanes) and the solvent was removed under reduced pressure to afford **1a** as a colorless liquid (21 g, 82%).

7,7,8,8,9,9,10,10,11,11,12,12,12-Tridecafluorododecan-1-ol, 2a. Iodide **6** (9.0 g, 17 mmol) was added to a flask containing $NaBH_4$ (2.5 g, 66 mmol) and DMSO (150 mL). The mixture was heated to 80 °C for 24 h under argon, poured slowly into 10% aqueous HCl, and extracted with hexanes (2 × 100 mL). The combined extracts were dried over $MgSO_4$ and the solvent was removed under reduced pressure. The residue was subjected to flash column chromatography (30:70 v/v ethyl acetate:hexanes) to afford **2a** as a colorless liquid (5.8 g, 84%). ^{1}H NMR (300 MHz, $CDCl_3$): δ 3.62 (t, $^3J_{HH}$ = 6.6 Hz, 2H, $-OCHH_2-$), 2.59 (bs, 1H, −OH), 1.94−2.12 (m, 2H), 1.38−1.82 (m). ^{13}C NMR (75 MHz, $CDCl_3$): δ 62.70 (C1), 32.41, 30.75 (t, $^3J_{CF}$ = 22 Hz, C6), 28.87, 25.40, 20.05. IR (ATIR): 3332 (br, O−H str), 2945, 2868, 1189 (C−O str), 1144, 1055, 845, 810, 731, 696, 654, 567, 534 cm^{-1}.

1-(Dodecyloxy)-4-(7,7,8,8,9,9,10,10,11,11,12,12,12-tridecafluorododecyloxy)benzene, 3a. 4-(Dodecyloxy)phenol (2.5 g, 9.0 mmol) was added to a solution of **2a** (5.7 g, 14 mmol) and PPh_3 (3.5 g, 14 mmol) in Et_2O (100 mL) in a dry flask under argon. Diethylazodicarboxylate, DEAD (2.5 mL, 13.6 mmol) was added dropwise by syringe and the mixture was stirred for 48 h. The mixture was poured into 10% aqueous NaOH (200 mL), and the resulting solution was extracted with Et_2O (2 × 100 mL). The combined extracts were dried over $MgSO_4$ and the solvent was removed under reduced pressure. The residue was purified by flash column chromatography (silica gel; 30:70 v/v CH_2Cl_2:hexanes) to afford **3a** as a colorless solid (3.08 g, 50%): mp = 60−64 °C. ^{1}H NMR (300 MHz, $CDCl_3$): δ 6.82 (s, 4H, Ar−H), 3.88−3.93 (m, 4H, $-OCHH_2-$), 1.98−2.16 (m, 2H, $-CF_2CH_2-$), 1.71−1.82 (m, 4H), 1.27−1.64 (m, 24H), 0.89 (t, $^3J_{HH}$ = 6.6 Hz, 3H, $-CH_3$). ^{13}C NMR (75 MHz, $CDCl_3$): δ 153.04 (Ar C−O), 115.37 (Ar C−H), 68.63, 68.26, 31.93, 30.81 (t, $^3J_{CF}$ = 22.8 Hz), 29.68, 29.65, 29.62, 29.44, 29.41, 29.36, 29.15, 28.86, 26.06, 25.78, 22.69, 20.08, 14.09. IR (ATIR): 2920 (Ar−H str), 2850, 1510, 1473, 1367, 1312, 1236, 1186, 1138 (C−O str), 1045, 825, 773, 698, 648, 571, 534, 453 cm^{-1}. HRMS: calcd for $C_{30}H_{41}F_{13}O_2$ = 680.28990; obsd = 680.28799; Δ = 2.8 ppm.

1-(Dodecyloxy)-4-(7,7,8,8,9,9,10,10,11,11,12,12,12-tridecafluorododecyloxy)-2,5-diiodobenzene, 4a. A solution of dialkoxybenzene **3a** (1.7 g, 2.6 mmol), iodine (1.2 g, 4.7 mmol), and KIO_3 (0.46 g, 2.2 mmol) in a mixture of acetic acid (30 mL), water (2 mL), and H_2SO_4 (0.5 mL) was heated to reflux for 48 h. The mixture was cooled, diluted with CH_2Cl_2 (100 mL) and washed with saturated aqueous Na_2SO_3 until the mixture turned clear. The organic layer was washed with 10% aqueous NaOH (2 × 50 mL), dried over $MgSO_4$, and the solvent was removed under reduced pressure. The residue was dissolved in a 40:60 v/v mixture of CH_2Cl_2 and hexanes and the solution was passed through a pad of silica. The solvent was removed under reduced pressure and the residue was recrystallized from isopropanol to afford **4a** as a colorless crystalline solid (1.6 g, 70%): mp = 48−52 °C. ^{1}H NMR (300 MHz, $CDCl_3$): δ 7.15 (s, 2H, Ar−H), 3.89−3.94 (m, 4H, $-OCHH_2-$), 1.98−2.16 (m, 2H, $-CF_2-CH_2-$), 1.73−1.85 (m, 4H), 1.25−1.69 (m, 24H), 0.86 (t, $^3J_{HH}$ = 7.2 Hz, 3H, $-CH_3$). ^{13}C NMR (75 MHz, $CDCl_3$): δ 153.08 (Ar C−O), 122.78 (Ar C−H), 86.28 (Ar C−I), 70.32, 69.96, 31.91, 30.78 (t, $^3J_{CF}$ = 22.8 Hz), 29.66, 29.57, 29.35, 29.26, 29.11, 28.87, 28.73, 26.01, 25.77, 22.68, 20.05, 14.11. IR (ATIR): 2922 (Ar−H str), 2854, 1485, 1464, 1348, 1207 (C−O str), 1144, 1051, 984, 845, 696, 654, 569, 528, 432 cm^{-1}. HRMS: calcd for $C_{30}H_{39}F_{13}I_2O_2$ = 932.08320; obsd = 932.08012; Δ = 3.3 ppm. Anal. Calcd: C, 38.64; H, 4.22; I, 27.22; O, 3.43; F, 26.49. Found: C, 38.80; H, 4.24; I, 27.38; O, 3.50; F, 26.41.

1-(Dodecyloxy)-2,5-diethynyl-4-(7,7,8,8,9,9,10,10,11,11,12,12,12-tridecafluorododecyloxy)benzene, 6a. Diiodide **4a** (1.5 g, 1.6 mmol) was added to a solution of $PdCl_2(PPh_3)_2$ (60 mg, 0.09 mmol) and CuI (20 mg, 0.11 mmol) in piperidine (19 mL). The mixture was degassed by freeze−pump−thaw and backfilled with argon. Trimethylsilane acetylene (0.57 mL, 4.0 mmol) was added dropwise over 10 min and the mixture was stirred for 24 h. CH_2Cl_2 (100 mL) was added and the solution was passed through a silica plug. The solvent was removed under reduced pressure to afford **5a** as a pale brown solid (1.23 g, 87%). ^{1}H NMR (300 MHz, $CDCl_3$): δ 6.89 (s, 2H, Ar−H), 3.92−3.97 (m, 4H, $-OCHH_2-$), 1.98−2.17 (m, 2H, $-CF_2CH_2-$), 1.74−1.86 (m, 4H), 1.26−1.66 (m, 24H), 0.88 (t, $^3J_{HH}$ = 7.2 Hz, 3H, $-CH_3$), 0.25 (s, 18H, −TMS). ^{13}C NMR (75 MHz, $CDCl_3$): δ 153.75 (Ar C−O), 117.12 (Ar C3−H), 113.85 (Ar C6−H), 100.95 (*C*≡C−TMS), 100.17 (C≡*C*−TMS), 69.37, 68.99, 31.91, 30.87 (t, $^3J_{CF}$ = 22.8 Hz), 29.62, 29.42, 29.32, 29.09, 28.89, 26.02, 25.75, 22.69, 20.14, 14.11, 0.01.

Tetra-*n*-butylammonium fluoride (1 M solution in THF, 2.5 mL, 2.5 mmol) was added dropwise to a solution of bis-(trimethylsilane) **5a** (0.98 g, 1.1 mmol) in dry THF (40 mL), the mixture was stirred for 1 h, and poured into H_2O (50 mL). The mixture was extracted with CH_2Cl_2 (100 mL), the combined extracts were dried over $MgSO_4$, and the solvent was removed under reduced pressure. The residue was recrystallized from ethanol to afford **6a** as a yellow powder (0.55 g, 67%): mp = 60−62 °C. ^{1}H NMR (300 MHz, $CDCl_3$): δ 6.95 (s, 1H, Ar−H), 6.94 (s, 1H, Ar−H), 3.94−4.00 (m, 4H, $-OCHH_2-$), 3.33 (s, 1H, ≡C−H), 3.32 (s, 1H, ≡C−H), 1.98−2.16 (m, 2H, $-CF_2CH_2-$), 1.75−1.87 (m, 4H), 1.26- 1.69 (m, 24H), 0.88 (t, $^3J_{HH}$ = 7.2 Hz, 3H, $-CH_3$). ^{13}C NMR (75 MHz, $CDCl_3$): δ 154.02 (Ar C−O), 117.64 (Ar C3−H), 113.17 (Ar C6−H), 82.65(*C*≡C−H), 79.68(C≡*C*−H), 69.59, 69.24, 31.91, 31.04 (t, $^3J_{CF}$ = 22.8 Hz), 29.66, 29.63, 29.57, 29.28, 29.08, 28.81, 28.73, 25.87, 25.62, 22.68, 14.11. IR (ATIR): 3309 (≡C−H str), 2922 (Ar−H str), 2854, 2108 (C≡C str), 1496, 1468, 1387, 1321, 1194 (C−O str), 1144, 1068, 856, 787, 696, 652, 606, 571, 530 cm^{-1}. HRMS: calcd for $C_{34}H_{41}F_{13}O_2$ = 728.28990; obsd = 728.29282; Δ = 4.0 ppm. Anal. Calcd: C, 56.04; H, 5.67; O, 4.39; F, 33.89. Found: C, 55.78; H, 5.73; O, 4.43; F, 34.01.

1-(Dodecyloxy)-4-(7,7,8,8,9,9,10,10,11,11,12,12,12-tridecafluorododecyloxy)-2-iodobenzene, 7a. 4-(Dodecyloxy)-3-iodophenol (4.4 g, 11 mmol) was added to a solution of **2a** (5.5 g, 13 mmol) and PPh_3 (3.43 g, 13.1 mmol) in Et_2O (100 mL) in a dry flask under argon. DEAD (2.4 mL, 13 mmol) was added dropwise via syringe and the solution was stirred for 48 h. The mixture was poured into 10% aqueous NaOH (200 mL) and the resulting solution was extracted with Et_2O (2 × 100 mL). The combined extracts were dried over $MgSO_4$ and the solvent was removed under reduced pressure. The residue was subjected to flash column chromatography (silica gel; 10:90 v/v EtOAc: hexanes) to afford **7a** as a white solid (6.64 g, 76%): m.p. = 39−41 °C. ^{1}H NMR (300 MHz, $CDCl_3$): δ 7.32 (d, $^4J_{ArH3\text{-}ArH5}$ = 2.7 Hz, 1H, Ar C3−H), 6.83 (dd, $^3J_{ArH5\text{-}ArH6}$ = 9 and $^4J_{ArH3\text{-}ArH5}$ = 2.7 Hz, 1H, Ar C5−H), 6.72 (d, $^3J_{ArH5\text{-}ArH6}$ = 9 Hz, 1H, Ar C6−H), 3.86−3.95 (m, 4H, $-OCHH_2-$), 1.98−2.16 (m, 2H, $-CF_2CH_2-$), 1.72−1.85 (m, 4H), 1.27−1.69 (m, 24H), 0.88 (t, $^3J_{HH}$ = 6.6 Hz, 3H, $-CH_3$). ^{13}C NMR (75 MHz, $CDCl_3$): δ 153.59 (Ar C−O), 152.20 (Ar C−O), 125.25, 115.37, 113.03 (Ar C−H), 86.95 (Ar C−I), 70.15, 68.44, 31.91, 30.79 (t, $^3J_{CF}$ = 22 Hz), 29.67, 29.57, 29.36, 29.33, 29.26, 29.03, 28.83, 26.08, 25.73, 22.69, 20.06, 14.12. IR (ATIR): 2916 (Ar C−H str, 2848, 1597, 1487, 1464, 1242, 1209 (C−O str), 1142, 1047, 1005, 866, 783, 694, 640, 571, 530 cm^{-1}. HRMS: calcd for $C_{30}H_{40}F_{13}IO_2$ = 806.18655; obsd = 806.18250; Δ = 5.0 ppm.

5-(Dodecyloxy)-2-(7,7,8,8,9,9,10,10,11,11,12,12,12-tridecafluorododecyloxy)-4-iodobenzaldehyde, 8a. $TiCl_4$ (46 mL of a 1 M solution in CH_2Cl_2, 46 mmol) was added in three portions to monoiodinated diether **7a** (6.2 g, 7.6 mmol) in dry flask at −40 °C under argon. The mixture was stirred for 15 min and dichloromethyl methyl ether (1.36 mL, 15.3 mmol) was added dropwise. The mixture was stirred for another 1.5 h at −40 °C and then poured into a mixture of 1 N HCl and ice. The mixture was extracted with CH_2Cl_2 (2 × 50 mL) and the combined organic extracts were washed with H_2O (100 mL), dried over $MgSO_4$. The solvent was removed under reduced pressure and the residue was subjected to column chromatography (silica gel, 30:70 CH_2Cl_2:hexanes) followed by recrystallization from isopropanol to afford **8a** as a colorless crystalline solid (2.72 g, 43%). Mp = 66−68 °C. ^{1}H NMR (300 MHz, $CDCl_3$): δ 10.39 (s, 1H, −CHO), 7.43 (s, 1H, ArC3−H), 7.16 (s, 1H, ArC6-H), 3.95−4.03 (m, 4H, $-OCHH_2-$), 1.97−2.15 (m, 2H, $-CF_2CH_2-$), 1.74−1.87 (m, 4H), 1.24−1.66 (m, 24H), 0.86 (t, $^3J_{HH}$ = 7.2 Hz). ^{13}C NMR (75 MHz, $CDCl_3$): δ 155.68 (Ar C−O), 152.20 (Ar C−O), 125.12 (Ar *C*−CHO), 124.45 (Ar C3−H), 108.87 (Ar C6−H), 96.73 (Ar C−I), 69.91, 69.12, 31.91, 30.77 (t, $^3J_{CF}$ = 22 Hz), 29.63, 29.57, 29.54, 29.34, 29.25, 28.99, 28.88, 28.79, 26.01, 25.75, 22.68, 20.09, 14.10. IR (ATIR): 2922 (Ar C−H str), 2852, 1676 (C=O str), 1591, 1464, 1390, 1321, 1209 (C−O str), 1144, 1039, 980, 872, 845, 791, 698, 654, 607, 571, 534, 449 cm^{-1}. HRMS: calcd for $C_{31}H_{40}F_{13}IO_3$ = 834.18146; obsd = 834.18235; Δ = 1.1 ppm.

1-(Dodecyloxy)-5-ethyny-4-(7,7,8,8,9,9,10,10,11,11,12,12,12-tridecafluorododecyloxy)-2-iodobenzene, 9a. The Bestman−Ohiro reagent (**10**) $(MeO)_2P(=O)C(=N_2)COCH_3$ (1.4 g, 7.3 mmol) was added dropwise to a mixture of aldehyde **8a** (2.5 g, 3.0 mmol) and K_2CO_3 (0.62 g, 4.5 mmol) in a 1:1 v/v mixture of anhydrous CH_2Cl_2 and MeOH (20 mL). The mixture was stirred for 48 h at room temperature, poured into 10% aqueous HCl (50 mL), and extracted with CH_2Cl_2 (2 × 50 mL). The combined organic extracts were dried over $MgSO_4$ and the solvent was removed under reduced pressure. The residue was recrystallized twice from isopropanol to afford **9a** as a colorless solid (1.58 g, 64%): mp = 59−61 °C. ^{1}H NMR (300 MHz, $CDCl_3$): δ 7.28 (s, 1H, ArC3-H), 6.86 (s, 1H, ArC6-H), 3.91−3.99 (m, 4H, $-OCHH_2-$), 3.28 (s, 1H, ≡C−H), 1.98−2.16 (m, 2H, $-CF_2CH_2-$), 1.75−1.86 (m, 4H), 1.26−1.69 (m, 24H), 0.88 (t, $^3J_{HH}$ = 6.6 Hz, 3H). ^{13}C NMR (75 MHz, $CDCl_3$): δ 154.87 (Ar C−O), 152.03 (Ar C−O), 124.00 (Ar C6−H), 116.93 (Ar C3−H), 112.49 (Ar C2), 88.53 (Ar C−I), 81.98 (**C**≡C−H), 79.85 (C≡**C**−H), 70.31, 69.76, 32.15, 31.00 (t, $^3J_{CF}$ = 22 Hz), 29.89, 29.80, 29.58, 29.52, 29.36, 29.07, 28.96, 26.27, 25.85, 22.93, 20.27, 14.34. IR (ATIR): 3313 (≡C−H str), 2924 (Ar C−H str), 2854, 1495, 1460, 1367, 1321, 1209 (C−O str), 1146, 1068, 984, 918, 850, 785, 748, 696, 654, 602, 569, 530 cm^{-1}. HRMS: calcd for $C_{32}H_{40}F_{13}IO_2$ = 830.18655; obsd = 830.18624; Δ = 0.4 ppm. Anal. Calcd: C, 46.28; H, 4.85; I, 15.28; O, 3.85; F, 29.74. Found: C, 46.06; H, 4.71; I, 15.42; O, 4.13; F, 29.48.

RgPPE(6,6/12). Monomer **9a** (551 mg, 663 μmol), was added to a mixture of toluene (8 mL) and piperdine (3 mL) followed by the addition of $Pd(PPh_3)_4$ (38 mg, 33 μmol) and then CuI (6.0 mg, 32 μmol). The mixture was degassed by two freeze/pump/thaw cycles and backfilled with argon. The solution was heated at 70 °C for 3 d, and poured into MeOH (50 mL) to precipitate the polymer. The solid was filtered from the mixture, dissolved in $CHCl_3$ (20 mL) and precipitated twice into acetone (100 mL). The resulting orange solid (358 mg, 77%) was dried under vacuum. ^{1}H NMR (300 MHz, $CDCl_3$): δ 7.02 (s, 1H, Ar−H), 7.01 (s, 1H, Ar−H), 4.03−4.08 (m, 4H, $-OCHH_2-$), 1.98−2.11 (m, 2H, $-CF_2CH_2-$), 1.80−1.89 (m, 4H), 1.26−1.68 (m, 24H), 0.87 (t, $^3J_{HH}$ = 6.9 Hz, 3H, $-CH_3$), see Results and Discussion. ^{13}C NMR (75 MHz, $CDCl_3$): δ 154.06, 153.69, 118.01, 91.63, 70.11, 31.91, 31.02 (t, $^3J_{CF}$ = 23.3 Hz), 29.65, 29.48, 29.33, 29.23, 28.98, 26.09, 25.81, 22.63, 20.27, 13.92. IR (ATIR): 2922 (Ar−H str), 2854, 2368 (C≡C str), 1516, 1471, 1431, 1419, 13232, 1215 (C−O str), 1144, 1074, 1051, 856, 700, 654, 569, 534 cm^{-1}.

RgPPE(8,4/12). Polymerization of monomer **9b** (462 mg) was performed according to the procedure provide above for the preparation of **RgPPE(6,6/12)** to afford **RgPPE(8,4/12)** as an orange solid (367 mg, 95%). ^{1}H NMR (300 MHz, $CDCl_3$): δ 7.01 (bs, 2H, ArH), 4.01−4.05 (m, 4H, $-OCHH_2-$), 1.97−2.11 (m, 2H, $-CF_2CH_2-$), 1.81−1.89 (m, 4H), 1.59−1.24 (m, 34H), 0.87 (t, $^3J_{HH}$ = 6.9 Hz, 3H, $-CH_3$). ^{13}C NMR (75 MHz, $CDCl_3$): δ 153.96 (Ar C−O), 117.96 (Ar C−H), 114.86 (Ar C−H), 91.64 (C≡C), 70.00, 31.93, 30.93 (t, $^3J_{CF}$ = 22.6 Hz), 29.09, 29.49, 29.27, 29.20, 26.09, 25.99, 22.65, 20.19, 13.98. IR (ATIR): 2924 (Ar−H str), 2854, 1516, 1510, 1431, 1419, 1390, 1217 (C−O str), 1132, 1010, 879, 854, 837, 719, 606, 534, 507 cm^{-1}.

RgPPE(10,2/12). Polymerization of monomer **9c** (390 mg) was performed in a mixture of toluene (3 mL) and diisopropylamine (1 mL) according to the procedure provided above for the preparation of **RgPPE(6,6/12)** to afford **RgPPE(10,2/12)** as an orange solid (268 mg, 87%). ^{1}H NMR (300 MHz, $CDCl_3$): δ 6.99 (bs, 2H), 3.99−4.03 (m, 4H), 1.91−2.00 (m, 2H), 1.79−1.86 (m, 4H), 1.23−1.55 (m, 32H), 0.85 (t, 3H *J* = 7.2 Hz). ^{13}C NMR (75 MHz, $CDCl_3$): δ 154.07 (Ar C−O), 118.43(Ar C−H), 115.15(Ar C−H), 91.90 (C≡C), 70.26, 32.05, 30.97 (t, $^3J_{CF}$ = 22.0 Hz), 29.79, 29.65, 29.62, 29.53, 29.34, 29.26, 26.23, 22.77, 20.44, 14.08. IR (ATIR): 2922 (Ar−H str), 2850, 2372 (C≡C str), 1516, 1514, 1434, 1419, 1278, 1193 (C−O str), 1043, 1045, 858, 812, 719, 534 cm^{-1}.

RnPPE(6,6/12). Monomers **4a** (463 mg, 497 μmol) and **6a** (362 mg, 497 μmol) were added to a mixture of toluene (8 mL) and diisopropylamine (2 mL), followed by the addition of $Pd(PPh_3)_4$ (29 mg, 25 μmol) and then CuI (5 mg, 26 μmol). The mixture was degassed by two freeze/pump/thaw cycles, the flask was backfilled with argon, and the solution was heated at 70 °C for 3 d. The mixture was poured into 50 mL of MeOH to precipitate the polymer. The solid was filtered from the mixture, dissolved in $CHCl_3$ and precipitated twice into acetone. The resulting orange solid (532 mg, 76%) was dried under vacuum. ^{1}H NMR (300 MHz, $CDCl_3$): δ 7.02 (bs, 2H, Ar−H), 4.01−4.11 (m, 4H, $-OCHH_2-$), 1.95−2.11 (m, 2H, $-CF_2CH_2-$), 1.80−1.91 (m, 4H), 1.25−1.67 (m, 24H), 0.87 (t, $^3J_{HH}$ = 6.9 Hz, 3H, $-CH_3$), see Results and Discussion. ^{13}C NMR (75 MHz, $CDCl_3$): δ 154.18 (Ar C−O), 153.85 (Ar C−O), 118.21 (Ar C−H), 115.14 (Ar C−H), 91.83 (C≡C), 70.27, 70.04, 32.03, 31.14 (t, $^3J_{CF}$ = 23.3 Hz), 29.77, 29.60, 29.35, 29.09, 26.20, 25.92, 22.74, 20.37, 14.02. IR (ATIR): 2929 (Ar−H str), 2858, 2368 (C≡C str), 1515, 1431, 1214 (C−O str), 1188, 1072, 858, 850, 696, 692, 571, 532 cm^{-1}.

RnPPE(8,4/12). Polymerization of monomers **4b** (406 mg, 472 μmol) and **6b** (313 mg, 472 μmol) was performed according to the procedure provided above for the preparation of **RnPPE-(6,6/12)** to afford **RgPPE(8,4/12)** as an orange solid (278 mg, 94%). ^{1}H NMR (300 MHz, $CDCl_3$): δ 7.01 (bs, 2H, ArH), 4.01−4.07 (m, 4H, $-OCHH_2-$), 1.96−2.11 (m, 2H, $-CF_2CH_2-$), 1.81−1.90 (m, 4H), 1.60−1.24 (m, 34H), 0.86 (t, $^3J_{HH}$ = 6.9 Hz, 3H, $-CH_3$). ^{13}C NMR (75 MHz, $CDCl_3$): δ 154.08 (Ar C−O), 118.42 (Ar C−H), 115.35 (Ar C−H), 91.61 (C≡C), 70.30, 32.04, 31.11 (t, $^3J_{CF}$ = 22.4 Hz), 29.80, 29.57, 29.45, 29.25, 26.21, 26.12, 22.75, 20.34, 14.05. IR (ATIR): 2927 (Ar−H str), 2856, 1516, 1471, 1431, 1390, 1381, 1217 (C−O str), 1132, 1026, 879, 858, 714, 607, 534, 501 cm^{-1}.

Acknowledgment. This research was supported by an award from the National Science Foundation (NSF-DMR-0347832). We also thank the Georgia Tech Center for Organic Photonics and Electronics (COPE) for support in the form of graduate fellowships to K.B.W. and R.N.

Supporting Information Available: Text giving synthesis and characterization information for homologues **b**−**e** of compounds **1-9** and figures showing the modification of substrates

and crystallographic data. This material is available free of charge via the Internet at http://pubs.acs.org.

References and Notes

(1) Xiao, X.; Nagahara, L. A.; Rawlett, A. M.; Tao, N. *J. Am. Chem. Soc.* **2005**, *127*, 9235–9240.
(2) Mwaura, J. K.; Pinto, M. R.; Witker, D.; Ananthakrishnan, N.; Schanze, K. S.; Reynolds, J. R. *Langmuir* **2005**, *21*, 10119–10126.
(3) Weder, C.; Sarwa, C.; Bastiaansen, C.; Smith, P. *Adv. Mater.* **1997**, *9*, 1035–1039.
(4) Francke, V.; Mangel, T.; Müllen, K. *Macromolecules* **1998**, *31*, 2447–2453.
(5) Weder, C.; Wrighton, M. S. *Macromolecules* **1996**, *29*, 5157–5165.
(6) Yang, J.-S.; Swager, T. M. *J. Am. Chem. Soc.* **1998**, *120*, 11864–11873.
(7) Fazio, D.; Mongin, C.; Donnio, B.; Galerne, Y.; Guillon, D.; Bruce, D. W. *J. Mater. Chem.* **2001**, *11*, 2852–2863.
(8) Breitenkamp, R. B.; Tew, G. N. *Macromolecules* **2004**, *37*, 1163–1165.
(9) Kim, J.; Swager, T. M. *Nature* **2001**, *411*, 1030–1034.
(10) Kim, J.; Levitsky, I. A.; McQuade, D. T.; Swager, T. M. *J. Am. Chem. Soc.* **2002**, *124*, 7710–7718.
(11) Clark, A. P-Z.; Cadby, A. J.; Shen, C. K-F.; Rubin, Y.; Tolbert, S. H. *J. Phys. Chem. B.* **2006**, *110*, 22088–22096.
(12) Ren, Y.; Lodge, T. P.; Hillmyer, M. A. *Macromolecules* **2001**, *34*, 4780–4787.
(13) Tran, H. V.; Hung, R. J.; Chiba, T.; Yamada, S.; Mrozek, T.; Hsieh, Y.-T.; Chambers, C. R.; Osborn, B. P.; Trinque, B. C.; Pinnow, M. J.; MacDonald, S. A.; Willson, C. G.; Sanders, D. P.; Conner, E. F.; Grubbs, R. H.; Conley, W. *Macromolecules* **2002**, *35*, 6539–6549.
(14) Robitaille, L.; Leclerc, M. *Macromolecules* **1994**, *27*, 1847–1851.
(15) Wang, J.; Ober, C. K. *Macromolecules* **1997**, *30*, 7560–7567.
(16) Johansson, G.; Percec, V.; Ungar, G.; Zhou, J. P. *Macromolecules* **1996**, *29*, 646–660.
(17) Hayakawa, T.; Wang, J.; Xiang, M.; Li, X.; Ueda, M.; Ober, C. K.; Genzer, J.; Sivaniah, E.; Kramer, E. J.; Fischer, D. A. *Macromolecules* **2000**, *33*, 8012–8019.
(18) Small, A. C.; Pugh, C. *Macromolecules* **2002**, *35*, 2105–2115.
(19) Wang, B.; Watt, S.; Hong, M.; Domercq, B.; Sun, R.; Kippelen, B.; Collard, D. M. *Macromolecules* **2008**, *41*, 5156–5165.
(20) Nambiar, R. R.; Brizius, G. L.; Collard, D. M. *Adv. Mater.* **2007**, *19*, 1234–1238.
(21) Nambiar, R.; Woody, K. B.; Ochocki, J. D.; Brizius, G. L.; Collard, D. M. *Macromolecules* **2009**, *42*, 43–51.
(22) Kotora, M.; Hácek, M.; Ameduri, B.; Boutevin, B. *J. Fluor. Chem.* **1994**, *68*, 49–56.
(23) Bonafoux, D.; Hua, Z.; Wang, B.; Ojima, I. *J. Fluor. Chem.* **2001**, *112*, 101–108.
(24) Brace, N. *J. Fluor. Chem.* **1982**, *20*, 313–327.
(25) Hong, X.; Tyson, J. C.; Middlecof, J. S.; Collard, D. M. *Macromolecules* **1999**, *32*, 4232–4239.
(26) Takeyama, Y.; Ichinose, Y.; Oshima, K.; Utimoto, K. *Tetrahedron Lett.* **1989**, *30*, 3159–3162.
(27) Delon, L.; Laurent, P.; Blancou, H. *J. Fluor. Chem* **2005**, *126*, 1487–1492.
(28) Moroni, M.; Le Moigne, J.; Luzzati, S. *Macromolecules* **1994**, *27*, 562–571.
(29) Xue, C.; Luo, F.-T. *Tetrahedron* **2004**, *60*, 6285–6294.
(30) Ofer, D.; Swager, T. M.; Wrighton, M. S. *Chem. Mater.* **1995**, *7*, 418–425.
(31) Bunz, U. H. F. *Chem. Rev.* **2000**, *100*, 1605–1644.
(32) Bunz, U. H. F.; Enkelmann, V.; Kloppenburg, L.; Jones, D.; Shimizu, K. D.; Claridge, J. B.; Loye, H.-C. Z.; Lieser, G. *Chem. Mater.* **1999**, *11*, 1416–1424.
(33) McIntosh, T. J.; Simon, S. A. *Biochemistry* **1993**, *32*, 8374–8384.
(34) Ionov, R.; Angelova, A. *Thin Solid Films* **1996**, *284−285*, 809–812.
(35) Takahashi, H.; Ohta, N.; Hatta, I. *Chem. Phys. Lipids* **2001**, *112*, 93–97.
(36) Ghosh, A. K.; Bischoff, A.; Cappiello, J. *Eur. J. Org. Chem.* **2003**, 821–832.